David Taylor Research Center
Bethesda, MD 20084–5000

DTRC–90/038 December 1990
Ship Structures and Protection Department
Research and Development Report

Transmission of a Shock Wave Across an Evacuated Barrier

by

George V. Waldo, Jr.

DTRC–90/038 Transmission of a Shock Wave Across an Evacuated Barrier

MAJOR DTRC TECHNICAL COMPONENTS

CODE 011 DIRECTOR OF TECHNOLOGY, PLANS AND ASSESSMENT

12 SHIP SYSTEMS INTEGRATION DEPARTMENT

14 SHIP ELECTROMAGNETIC SIGNATURES DEPARTMENT

15 SHIP HYDROMECHANICS DEPARTMENT

16 AVIATION DEPARTMENT

17 SHIP STRUCTURES AND PROTECTION DEPARTMENT

18 COMPUTATION, MATHEMATICS & LOGISTICS DEPARTMENT

19 SHIP ACOUSTICS DEPARTMENT

27 PROPULSION AND AUXILIARY SYSTEMS DEPARTMENT

28 SHIP MATERIALS ENGINEERING DEPARTMENT

DTRC ISSUES THREE TYPES OF REPORTS:

1. **DTRC reports, a formal series,** contain information of permanent technical value. They carry a consecutive numerical identification regardless of their classification or the originating department.

2. **Departmental reports, a semiformal series,** contain information of a preliminary, temporary, or proprietary nature or of limited interest or significance. They carry a departmental alphanumerical identification.

3. **Technical memoranda, an informal series,** contain technical documentation of limited use and interest. They are primarily working papers intended for internal use. They carry an identifying number which indicates their type and the numerical code of the originating department. Any distribution outside DTRC must be approved by the head of the originating department on a case-by-case basis.

NDW-DTNSRDC 5602/51 (Rev 2-88)

REPORT DOCUMENTATION PAGE

1a. REPORT SECURITY CLASSIFICATION: UNCLASSIFIED	1b. RESTRICTIVE MARKINGS
2a. SECURITY CLASSIFICATION AUTHORITY	3. DISTRIBUTION/AVAILABILITY OF REPORT: Approved for public release; distribution is unlimited.
2b. DECLASSIFICATION/DOWNGRADING SCHEDULE	
4. PERFORMING ORGANIZATION REPORT NUMBER(S): DTRC-90/038	5. MONITORING ORGANIZATION REPORT NUMBER(S)
6a. NAME OF PERFORMING ORGANIZATION: David Taylor Research Center; 6b. OFFICE SYMBOL (If applicable): Code 175.2	7a. NAME OF MONITORING ORGANIZATION: David Taylor Research Center, Independent Exploratory Development (IED) Program
6c. ADDRESS (City, State, and ZIP Code): Bethesda, MD 20084-5000	7b. ADDRESS (City, State, and ZIP Code): Bethesda, Maryland 20084-5000
8a. NAME OF FUNDING/SPONSORING ORGANIZATION: Independent Exploratory Development; 8b. OFFICE SYMBOL (If applicable)	9. PROCUREMENT INSTRUMENT IDENTIFICATION NUMBER
8c. ADDRESS (City, State, and ZIP Code)	10. SOURCE OF FUNDING NUMBERS

PROGRAM ELEMENT NO.	PROJECT NO.	TASK NO.	WORK UNIT ACCESSION NO.
62936N			DN500071

11. TITLE (Include Security Classification): Transmission of a Shock Wave Across an Evacuated Barrier

12. PERSONAL AUTHOR(S): Waldo, Jr., George V.

13a. TYPE OF REPORT	13b. TIME COVERED	14. DATE OF REPORT (YEAR, MONTH, DAY)	15. PAGE COUNT
Final	FROM 891001 TO 901001	1990, December	52

16. SUPPLEMENTARY NOTATION

17. COSATI CODES			18. SUBJECT TERMS (Continue on reverse if necessary and identify by block number)
FIELD	GROUP	SUB-GROUP	Shock Waves, Attenuation, Cavitation, Protection, Transmission, Bubble Screen

19. ABSTRACT (Continue on reverse if necessary and identify by block number)

The transmission of a one-dimensional shock wave across an evacuated barrier in a liquid is modeled. In this model the interaction of the shock wave with the incident side of the barrier causes the liquid to cavitate. The cavitated liquid then moves across the barrier and collides with the liquid on the opposite side of the barrier, thus setting in motion a transmitted wave.

The pressure history of the transmitted wave is determined from that of the incident shock wave. Although the impulse of the transmitted wave is the same as that of the incident shock wave, the transmitted wave can have considerably lower peak pressure and energy flux density. Possible extensions of this model are discussed. Also, potential mililtary and industrial applications are considered.

20. DISTRIBUTION/AVAILABILITY OF ABSTRACT: ☐ UNCLASSIFIED/UNLIMITED ☒ SAME AS RPT ☐ DTIC USERS	21. ABSTRACT SECURITY CLASSIFICATION: UNCLASSIFIED
22a. NAME OF RESPONSIBLE INDIVIDUAL: George V. Waldo, Jr.	22b. TELEPHONE (Include Area Code): (301) 227-1782; 22c. OFFICE SYMBOL: Code 1750.2

DD FORM 1473, JUN 86 *Previous editions are obsolete.*

CONTENTS

FIGURES

Page

ROMAN NOTATION

c	speed of sound in liquid
D	barrier thickness
D^*	nondimensional barrier thickness
E_I	energy flux density of incident shock wave
E_T	energy flux density of transmitted wave
f	incident shock wave pressure function
P_I	pressure of incident shock wave
P_T	pressure of transmitted wave
P_v	pressure in cavity
P_0	total pressure for reflection at $x = 0$
P_1	total pressure for reflection at $x = x_1$
t	time after arrival of incident shock wave
t'_n	arrival time of n-th pulse in limit of zero barrier thickness
t''_n	arrival time of n-th pulse
V_n	velocity of n-th cavitated slab
$V(x)$	velocity of liquid cavitated at x
x	location relative to incident (left) side of barrier
x_n	location of n-th cavitation
z	any real number ≥ 0

GREEK NOTATION

δ	small real number ≥ 0, i.e., $\delta \approx 0.0261$
ϵ	any real number > 0
θ	time-decay constant of incident shock wave
ρ	mass density of liquid
τ	cut-off time of hyperbolically decaying shock wave

THIS PAGE INTENTIONALLY LEFT BLANK

ABSTRACT

The transmission of a one-dimensional shock wave across an evacuated barrier in a liquid is modeled. In this model the interaction of the shock wave with the incident side of the barrier causes the liquid to cavitate. The cavitated liquid then moves across the barrier and collides with the liquid on the opposite side of the barrier,thus producing a transmitted wave into the liquid.

The pressure history of the transmitted wave is determined from that of the incident shock wave. Although the impulse of the transmitted wave is the same as that of the incident shock wave, the transmitted wave can have considerably lower peak pressure and energy flux density. Possible extensions of this model are discussed. Also, potential military and industrial applications are considered.

ADMINISTRATIVE INFORMATION

This work was funded by the David Taylor Research Center Independent Exploratory Development (IED) program under Work Unit 1750-236 for FY-1990.

INTRODUCTION

Surface ships and submarines must be protected from underwater explosions so that they can survive to accomplish their missions. Furthermore, it is important that the effects of underwater explosions in industrial applications (such as underwater construction and demolition) be contained in the desired region so that machinery and personnel are protected. One method of protection is to place a barrier between an explosion and an object to reduce the damaging effects of the shock wave. This barrier might consist of a foam or bubble screen or some more

complicated arrangement. However, to find the proper types of barriers it is first necessary to understand the fundamental mechanisms that reduce the damage. To achieve this it is worthwhile to examine and analyze simple models of protective barriers to identify and to model mathematically the physics of the phenomena. It is the objective of this program to develop such a model. In this model a simple one-dimensional shock wave is incident on a barrier containing *no* material, i.e., a *vacuum*. The development of the model considers the cavitation of the liquid at its interface with the barrier. This development shows that the decay in the pressure of the incident wave causes a reduction in the pressure and energy flux per unit area of the transmitted wave. Of course, there is no loss of energy to the vacuum itself. Previous work on the transmission of shock waves across barriers (composed of foam, air bubbles, etc.) appears to have concentrated on the transmission across the material *inside* the barrier rather than considering the effect of the liquid *cavitating at the interface* of the liquid with the barrier, see, e.g., Refs. 1-10. However, some work considering cavitation has been performed, see, e.g., Lyakhov.[11] It is plausible that existing experimental data that were obtained for bubble screens can be used to test this theory.

EVACUATED-BARRIER CAVITATION MODEL

In the evacuated-barrier cavitation model, a one-dimensional planar shock wave propagating in a liquid is incident on a barrier that is immersed in the liquid; see Fig. 1. The pressure in the shock wave is sufficiently high so that the pressure in the barrier is

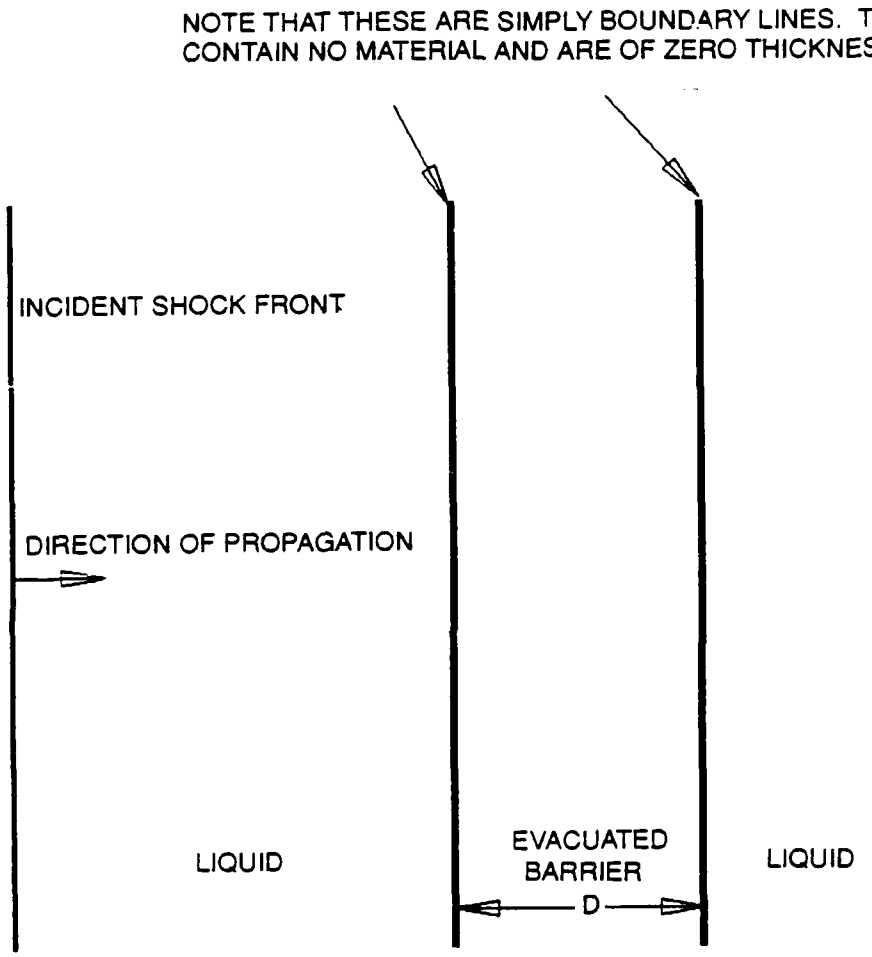

Fig. 1. Evacuated–barrier model.

negligible in comparison to that of the shock wave. Thus, the pressure within the barrier can be considered as that of a vacuum, i.e., zero. If the incident pressure is sufficiently high, the reflected shock wave will cause a quasi-continuous cavitation of the liquid. This will result in a region of cavitation bubbles between the front of the reflected shock wave and the barrier as shown in Fig. 2. The cavitated liquid parcels* will then move to the opposite side of the barrier and collide with it. The shock wave resulting from these collisions will subsequently propagate into the liquid on the other side of the barrier, as shown in Fig. 3. However, the times of arrival of the liquid parcels are spread out because of their movement across the barrier. This spread causes the shock wave that they produce to have a considerably lower pressure than that of the incident shock wave. A similar reduction occurs in the energy flux density of the shock wave.

REVIEW OF THEORY FOR INITIAL VELOCITY OF CAVITATED LIQUID

It is instructive to review the theory for determining the velocity distribution in the liquid immediately after cavitation. This review is similar to work that has been reported by, e.g., Kennard,[12] Cushing,[13] and Waldo.[14] Consider a one-dimensional situation where a planar shock wave is acoustically propagating the x- direction but in the domain where x is negative and is incident on a free surface at x = 0 as shown in Fig. 4. Also let

---

*For one-dimensional flow, these parcels are "slabs," as portrayed in Fig. 3 and for three-dimensional flow they might be droplets.

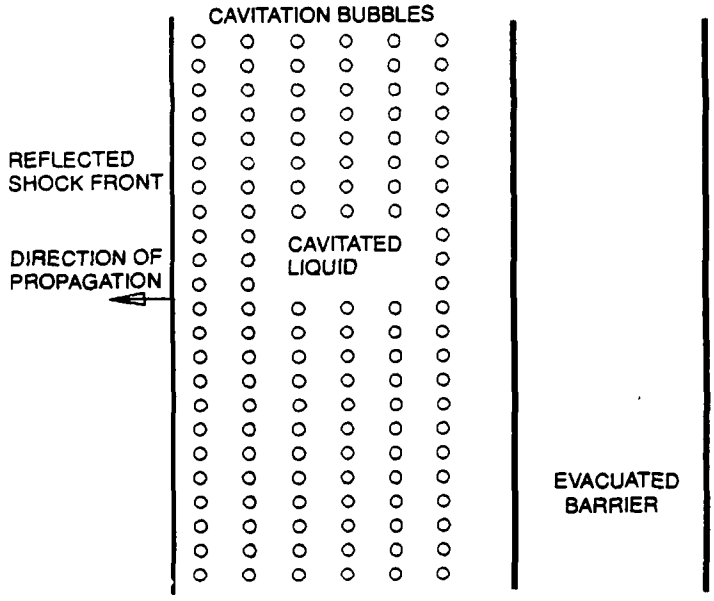

Fig. 2. Cavitation.

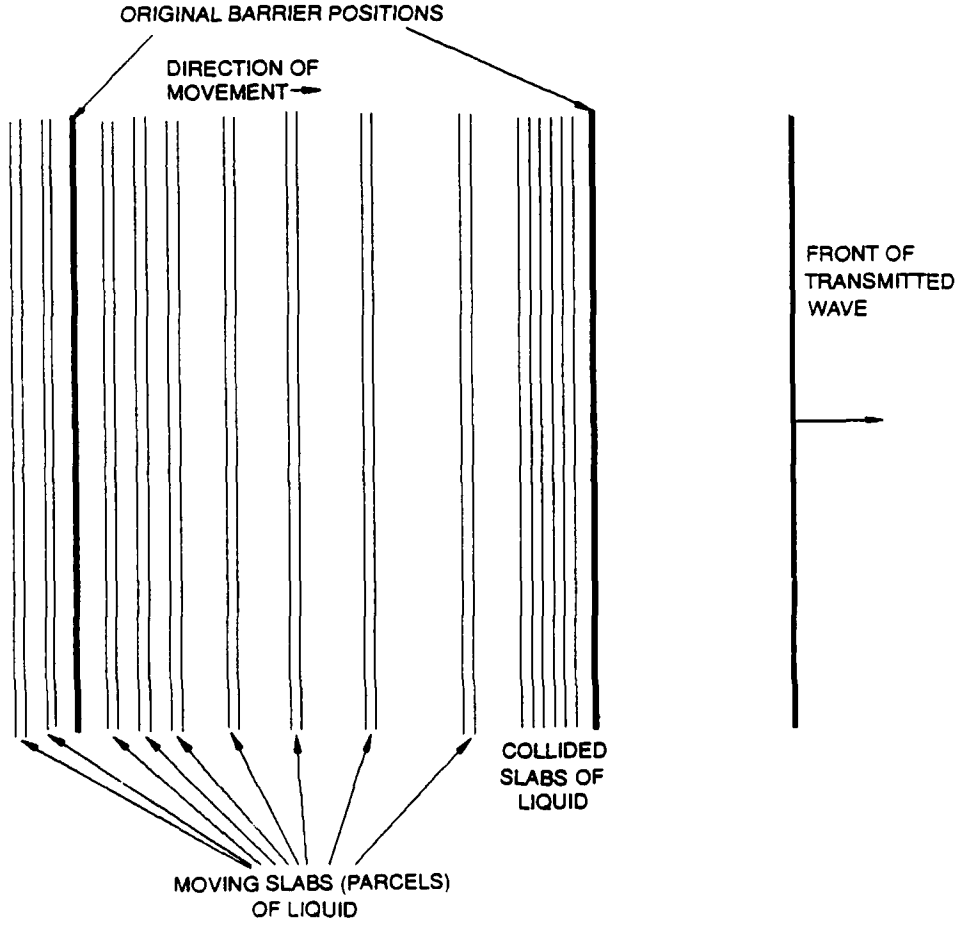

Fig. 3. Collision of cavitated slabs and transmitted wave.

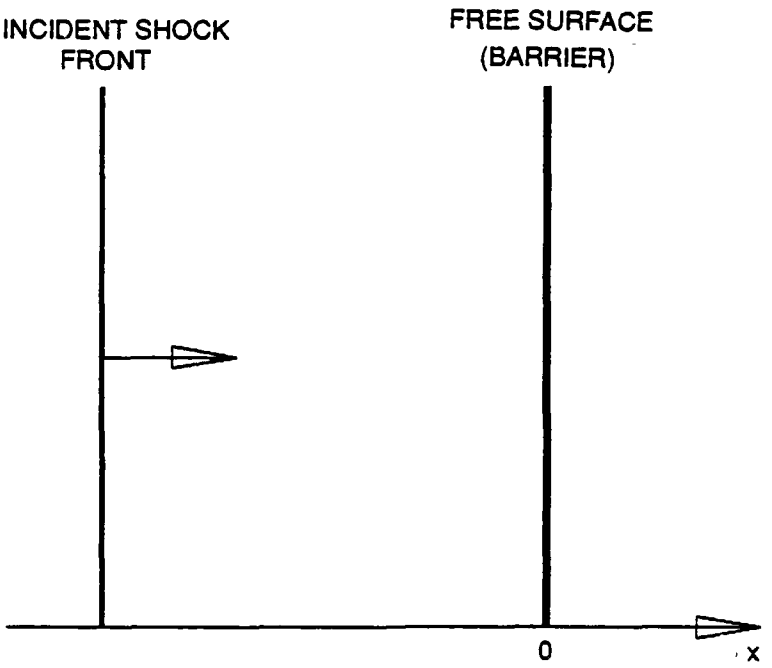

Fig. 4. Planar shock wave incident on surface.

the pressure of this incident shock wave at the location x and time t be given by

$$P_I(x,t) = f(ct - x), \quad \text{for } ct \geq x$$
$$= 0, \quad \text{for } ct < x, \qquad (1)$$

where c is the speed of sound in the liquid (see, e.g., Cole,[15] p. 143 or Landau and Lifshitz,[16] p. 247). From this equation it is seen that this shock wave arrives at the free surface at t = 0. Now let the pressures in the incident wave be sufficiently large so that the pressure at the free surface and the hydrostatic pressure are negligible in comparison. Immediately after arrival, a reflected wave will propagate from the free surface in opposite direction with the pressure

$$- f(ct + x), \quad \text{for } ct \geq -x$$

and

$$0, \quad \text{for } ct < -x;$$

see Fig. 5. Thus, if the pressures of the incident wave are positive, then the reflected wave is a tension wave. In this situation, the total pressure in the liquid will be the pressure of the incident wave plus the pressure of the reflected wave, i.e.,

$$P_0(x,t) = f(ct - x) - f(ct + x), \quad \text{for } ct \geq -x, \qquad (2)$$

where the "0" in the subscript denotes that the reflection is at the free surface at x = 0. Note that Eq. 2 obeys the boundary condition, $P_0(0,t) = 0$, at the free surface (at x = 0). It is

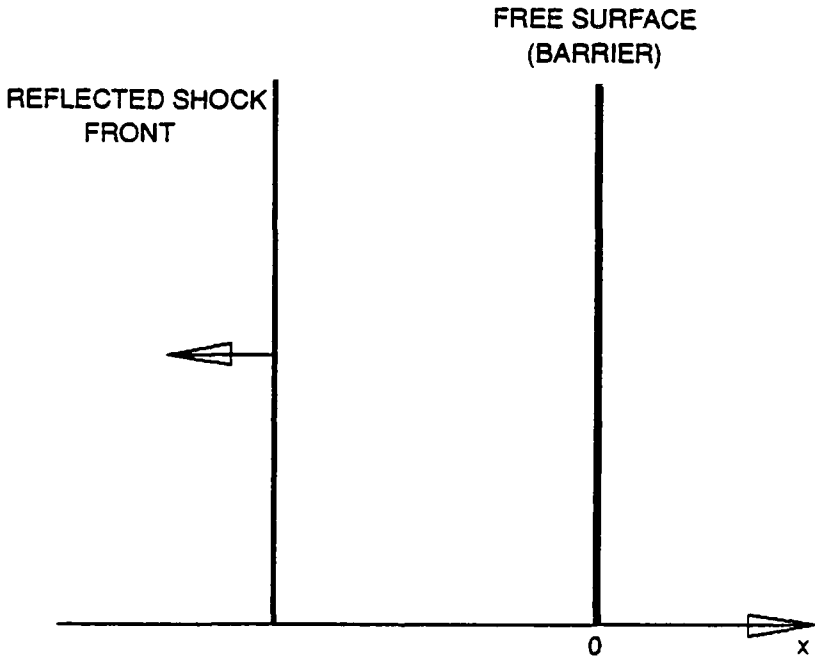

Fig. 5. Reflected shock wave.

now assumed that f(z) is a *decreasing* function of z. That is, for any real number $z \geq 0$,

$$f(z + \epsilon) < f(z), \text{ for any real number } \epsilon > 0,$$

see Fig. 6. For this decreasing function it is seen that for $x<0$

$$P_0(x,t) < 0, \quad \text{for } ct \geq -x.$$

Now let the pressures in the incident wave be sufficiently large so that the magnitude of the (negative) pressure* necessary to cause the liquid to cavitate is also negligible in comparison. Under this condition the liquid will cavitate and form a pair of new free surfaces at $x = x_1$ that are very close to the original free surface (at $x = x_0 = 0$); see Eq. 2 for the total pressure in the liquid. The very small space between this pair of new free surfaces is the first cavity; see Fig. 7. Defining ρ to be the mass density of the liquid and using one-dimensional linear acoustic theory (see, e.g., Cole,[15] p. 143 or Landau and Lifshitz,[16] p. 247), it is seen that the velocity of the liquid at the new free surface that is closest to the barrier on this cavity, occurring at $t = -x_1/c$, is

$$\begin{aligned} V_1 &= [f(ct - x_1) + f(ct + x_1)]/(\rho c) \\ &= [f(-2x_1) + f(0)]/(\rho c) \\ &\approx 2f(-2x_1)/(\rho c), \end{aligned} \tag{3}$$

because x_1 is approximately zero and becomes exactly zero in the

---

*The problem for lower pressures is much more complicated, see, e.g., Prosperetti [17].

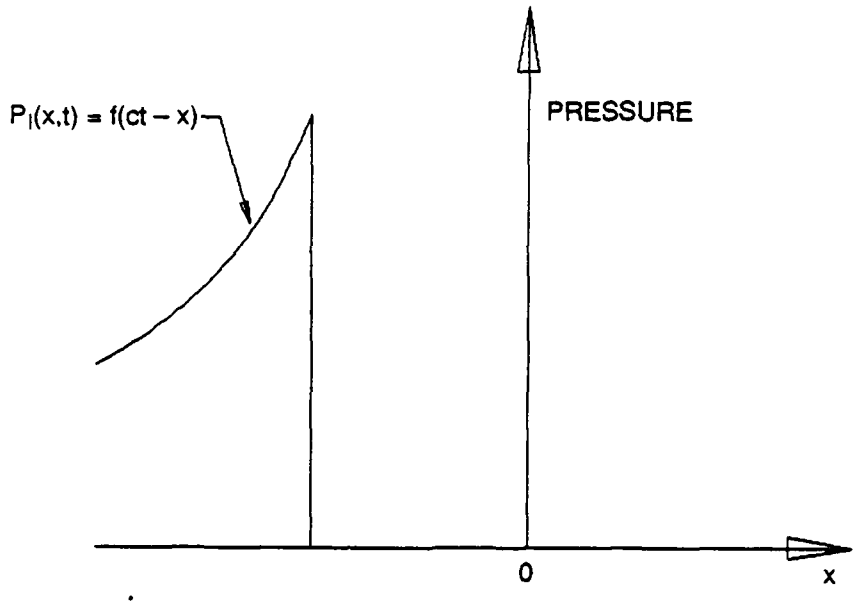

Fig. 6. Decreasing incident shock wave.

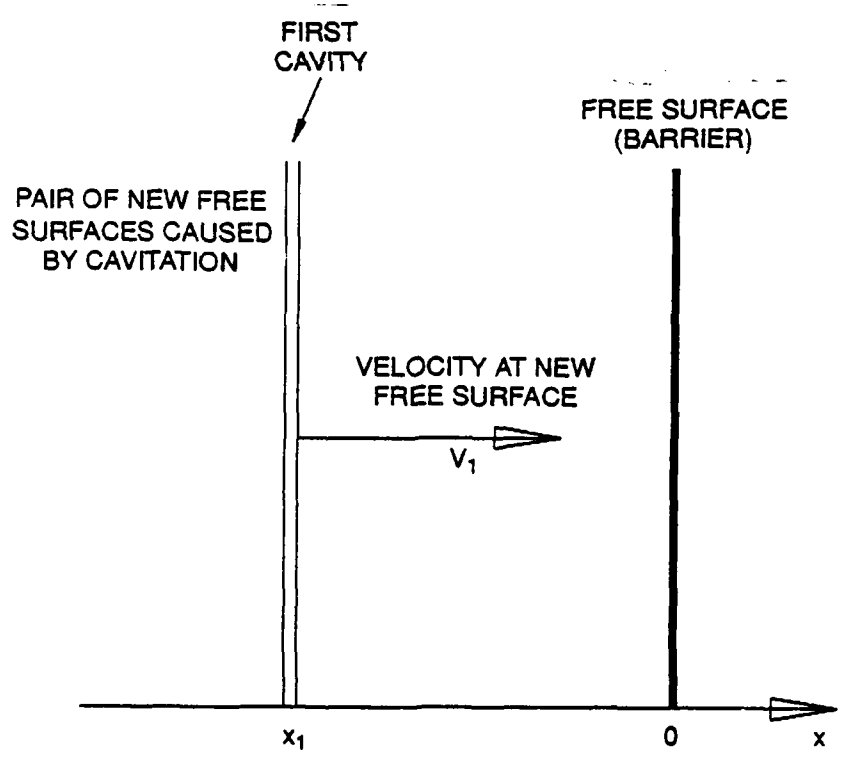

Fig. 7. Pair of new free surfaces caused by cavitation.

limit of zero cavitation pressure at the free surface. Because the space between the slabs is negligibly small immediately after cavitation, the location of *both* surfaces is at $x = x_1$. It is noted that, for this *first* new cavitated slab, the approximation

$$V_1 \approx 2f(0)/(\rho c) \qquad (4)$$

could also be used and would be exact in the limit of zero cavitation pressure.

In similar fashion, the remainder of the incident wave will reflect off of this first cavity with the pressure

$$- f(ct + x - 2x_1) + P_v, \text{ for } ct \geq - x \text{ and } x \leq x_1,$$

where P_v is the pressure in the cavity (that might be of similar magnitude to the vapor pressure of the liquid). The total pressure in the liquid will be the pressure of the incident wave plus the pressure of the reflected wave, i.e.,

$$P_1(x,t) = f(ct - x) + [-f(ct + x - 2x_1) + P_v],$$
$$\text{for } ct \geq - x \text{ and } x \leq x_1,$$

where the subscript "1" denotes that the reflection is at $x = x_1$. It is noted that this equation obeys the boundary condition, $P_1(x_1,t) = P_v$ at $x = x_1$. Now let the pressures in the incident wave be sufficiently large so that P_v is also negligible in comparison. Under this condition the liquid will cavitate and form a *second* pair of new free surfaces, see Fig. 8, at $x = x_2$ that are very close to the first pair (at $x = x_1$). The velocity of the liquid at the new free surface that is closest to the barrier on this second cavity, occurring at $t = - x_2/c$, is

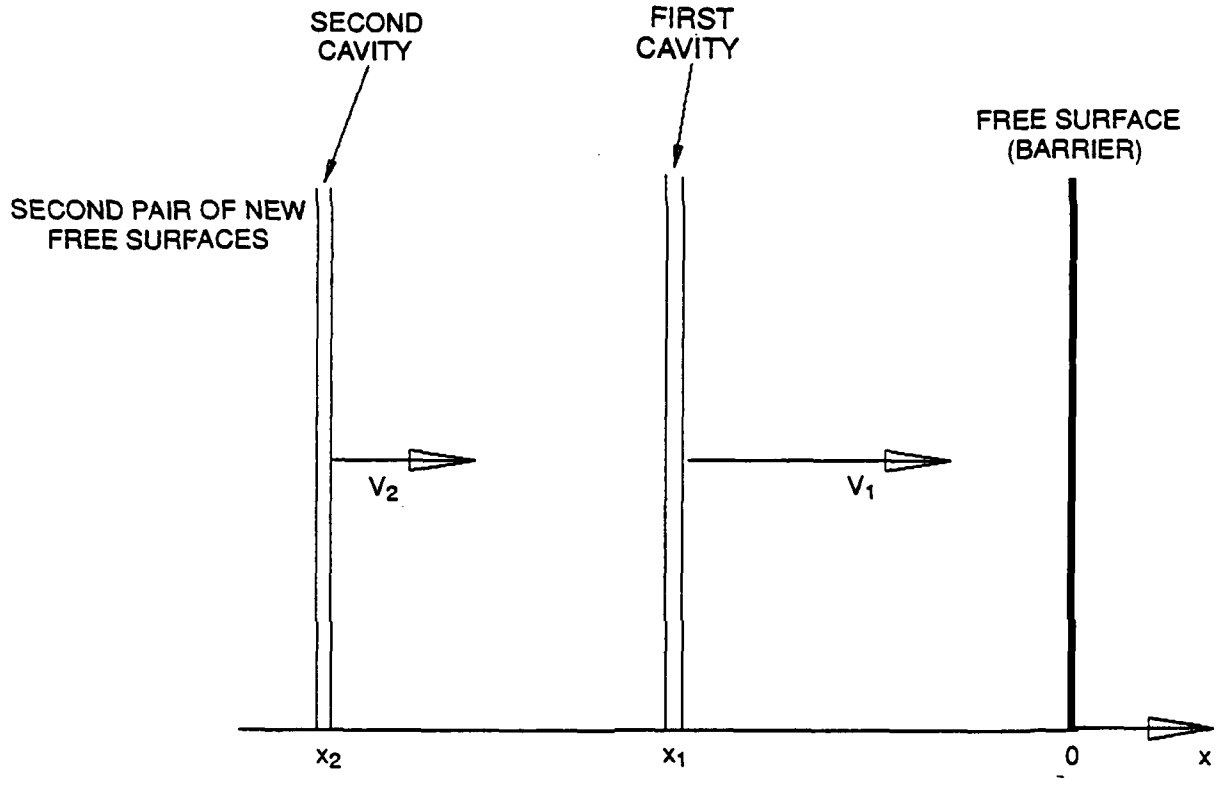

Fig. 8. Second pair of new free surfaces caused by cavitation.

$$V_2 = [f(ct - x_2) + f(ct + x_2 - 2x_1)]/(\rho c)$$
$$= [f(-2x_2) + f(- 2x_1)]/(\rho c)$$
$$\approx 2f(-2x_2)/(\rho c), \qquad (5)$$

because $x_2 \approx x_1$ and becomes exactly equal in the *limit* of both zero cavitation pressure and P_v.

As long as the pressure in the incident wave is sufficiently large, this process of successive cavitations and new free surfaces will continue so that we can consider the n-th cavitation in a similar fashion; see Fig. 9. The incident wave will reflect off of this n-th cavity with the pressure

$$- f(ct + x - 2x_n) + P_v, \quad \text{for } ct \geq -x \text{ and } x \leq x_n.$$

It is obvious from the previous discussion that the total pressure obeys the boundary condition at $x = x_n$. For sufficiently high pressures in the incident wave, the liquid will cavitate and form an n+1-th pair of new free surfaces at $x = x_{n+1}$ that is very close to the n-th pair (at $x = x_n$). The velocity of the liquid at the new free surface on this n+1-th cavity occurring at $t = -x_{n+1}/c$ is

$$V_{n+1} = [f(ct - x_{n+1}) + f(ct + x_{n+1} - 2x_n)]/(\rho c)$$
$$= [f(-2x_{n+1}) + f(- 2x_n)]/(\rho c)$$
$$\approx 2f(-2x_{n+1})/(\rho c), \qquad (6)$$

because $x_{n+1} \approx x_n$ and becomes exactly equal in the *limit* of zero cavitation pressure and P_v.

The liquid between these cavitated surfaces can be regarded as cavitated "slabs"; see Fig. 9. Because the distances between

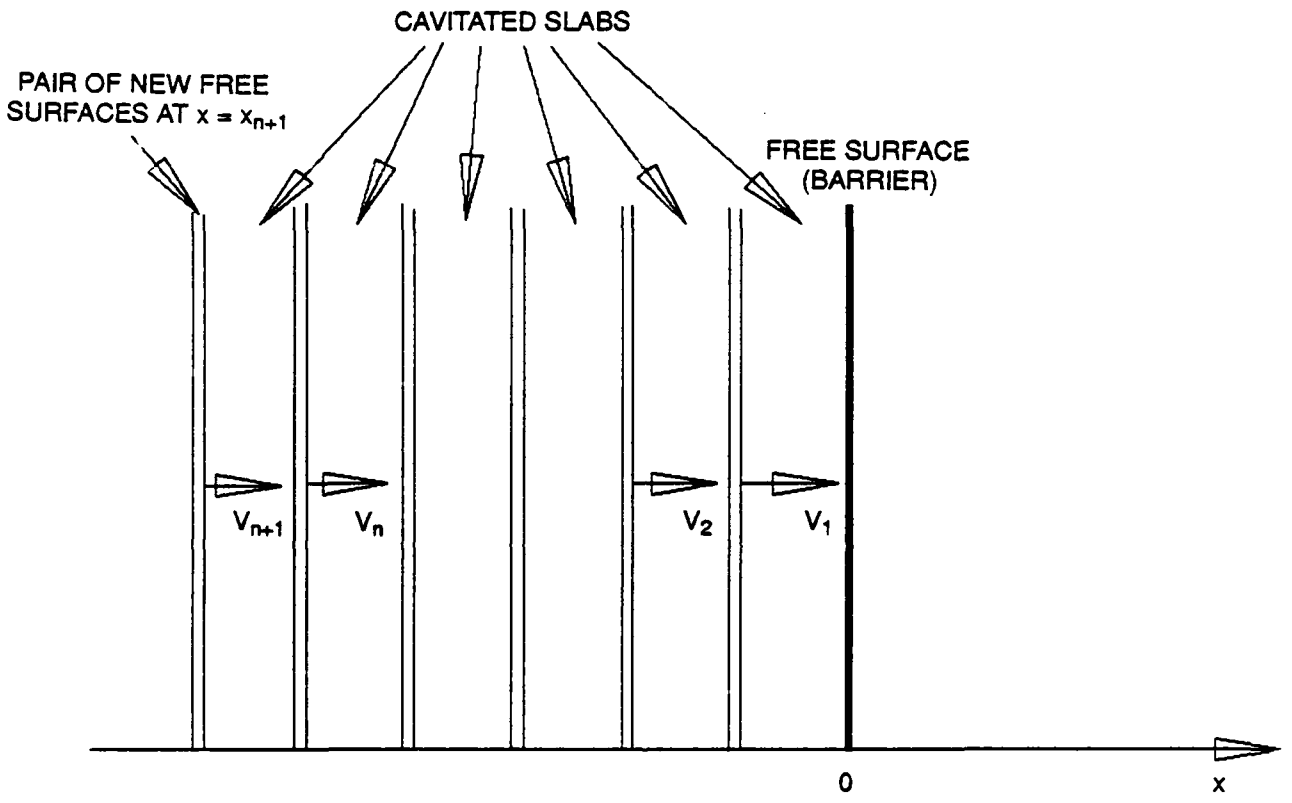

Fig. 9. Pair of new free surfaces at $x = x_{n+1}$.

the cavitated surfaces are very small, the slabs are very thin; and, because they are very thin, the slabs have approximately uniform velocity throughout their thicknesses. Thus, the approximate velocity of the n+1-th slab given by Eq. 6 is exact in the limit where the cavitation pressure and P_v are zero. It is mentioned in passing that Eq. 6 can also be derived by dividing the impulse per unit area imparted by the incident wave to the n+1-th slab, i.e.,

$$f(-2x_{n+1})[2(x_n - x_{n+1})/c],$$

by the mass per unit area of the slab, i.e.,

$$\rho(x_n - x_{n+1}),$$

as was done by Waldo,[14] pp. 2 and 3. It is now convenient to define the velocity function V(x) as

$$V(x) = 2f(-2x)/(\rho c), \tag{7}$$

from which

$$V(x_n) \approx V_n \tag{8}$$

by using Eq. 6 for the velocity of the slab.

TRANSMITTED WAVE

After the first slab cavitates, it moves across the barrier and collides with the opposite side of the barrier; see Fig. 10. This collision produces an acoustic pulse that propagates into the liquid on the opposite side of the barrier. In the acoustic limit, the displacement of the liquid in the slab after collision

is negligible so that the position of the end (i.e., the left-hand side in Fig. 10) of the first slab remains at $x = D+x_1$ (remember that $x_1 < 0$) . In like manner, after the second slab cavitates, it also moves across the barrier and collides with the first slab (that has previously collided with the opposite side of the barrier and, in the acoustic limit, has the same thickness as when it was formed by cavitation); see Fig. 11. This process continues so that after n-1 succeeding slabs pile up on each other, the n-th slab collides with the pile of n-1 slabs at the time,

$$(-x_n/c) + (D/V_n),$$

where D is defined to be the barrier thickness (see discussion of Eq. 6 for the velocity of the slab). The time when the acoustic pulse from this collision arrives at x = D (i.e., the opposite side of the original position of the barrier; see Fig. 12) is (see Eq. 8)

$$\begin{aligned} t''_n &= [(-x_n/c) + (D/V_n)] + (-x_n/c) \\ &\approx (-2x_n/c) + [D/V(x_n)] \\ &= t'_n + D/V(-ct'_n/2), \end{aligned} \tag{9}$$

where

$$t'_n = -2x_n/c \tag{10}$$

is the arrival time of the pulse in the limit of zero barrier thickness. It can be seen, using Eq. 1 for the pressure of the incident shock wave, that

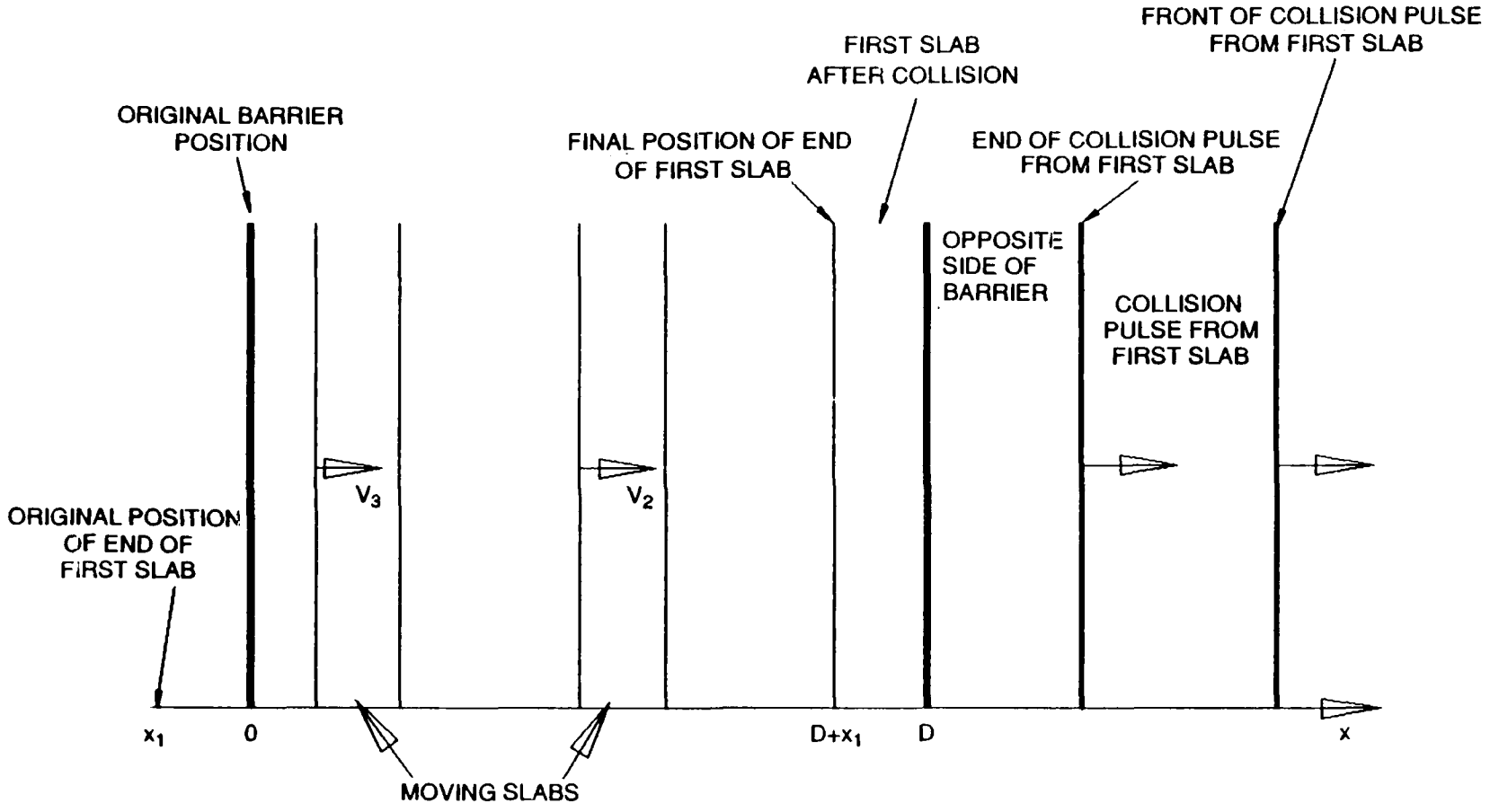

Fig. 10. Collision of first slab with the opposite side of the barrier.

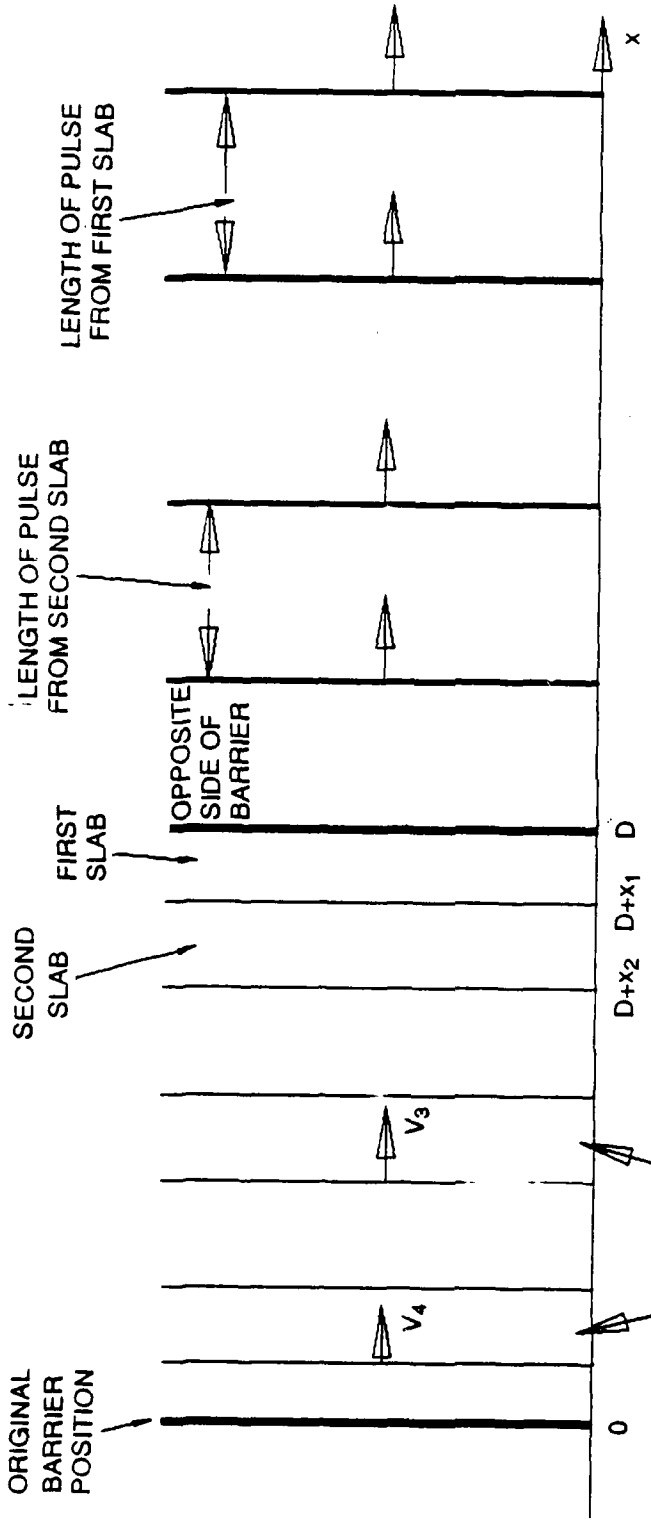

Fig. 11. Collision of the second slab with the first slab.

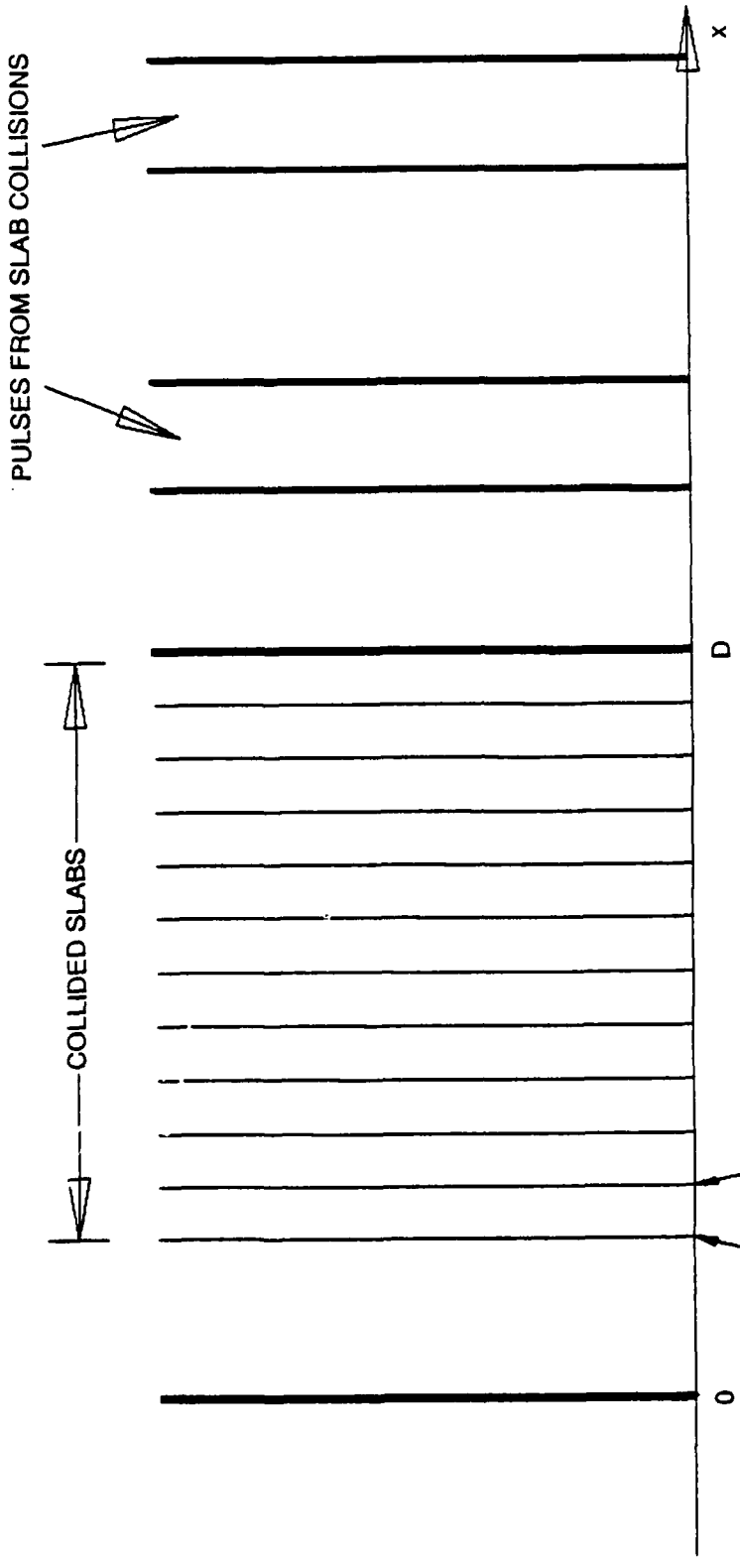

Fig. 12. Collision of the n+1–th slab with the n–th slab.

$$f(ct'_n) = P_I(0,t'_n). \tag{11}$$

Substituting Eq. 11 into Eq. 7, the velocity function, gives

$$V(-ct'_n/2) = 2P_I(0,t'_n)/(\rho c). \tag{12}$$

Substituting Eq. 12 into Eq. 9, for the time when the acoustic pulse from this collision arrives at x = D, yields

$$t''_n \approx t'_n + \tfrac{1}{2}\rho cD/P_I(0,t'_n). \tag{13}$$

From this equation, it is seen that it is appropriate to define the functional t'' such that, in the limit of zero slab thickness,

$$t''_n = t''(t'_n), \tag{14}$$

or simply

$$t'' = t''(t'). \tag{15}$$

Differentiation of Eq. 15 yields

$$\frac{dt''}{dt'} = 1 - \tfrac{1}{2}\rho cD[P_I(0,t')]^{-2}\,\frac{d}{dt'}P_I(0,t'). \tag{16}$$

This equation implies that $dt''/dt' > 1$, for $D > 0$, because $P_I(0,t')$ is a *decreasing* function of t'. This result is expected because the fact that the pressure of the incident shock wave decreases with time implies that the cavitated slabs have successively decreasing velocities. This causes a spread in their arrival times at the opposite side of the barrier resulting in $dt''/dt' > 1$.

If the slabs were of finite thickness, then the transmitted wave would consist of a series of pulses, each corresponding to a slab collision; see Fig. 12. However, in the limit of zero thickness slabs (that occur for sufficiently high pressure incident shock waves, as explained previously) these pulses are of zero duration and of infinite frequency. In this situation the pulses are rapidly damped out by viscous effects so that the transmitted wave becomes a smooth function of time such that the *momentum of each pulse is conserved*, but there might be a significant loss of energy. It is emphasized that the loss of energy occurs in the *liquid*, as it must because there is a vacuum within the barrier itself. Using Eq. 10 for the pulse arrival time in the limit of zero barrier thickness and Eq. 12 for the velocity function, it can be easily seen that the momentum per unit area of the n+1-th slab is

$$\begin{aligned} \rho(x_n - x_{n+1})V_{n+1} &\approx P_I(0,t'_{n+1})(t'_{n+1} - t'_n) \\ &= P_I(0,t')dt', \end{aligned} \tag{17}$$

where $t' = t'_{n+1}$ and $dt' = t'_{n+1} - t'_n$ in the limit of zero thickness slabs. Integration of this equation over time to a given value of t' provides the total momentum of the collided slabs up to t'. This total momentum is equal to the total impulse of the incident shock wave up to t'. This total momentum must be equal to the total impulse up to $t'' = t''(t')$ of the *transmitted* wave at x = D, i.e.,

$$\int_0^{t'} P_I(0,t)dt = \int_0^{t''} P_T(D,t)dt,$$

where $P_T(x,t)$ is the pressure of the transmitted wave at any location, x, and at any time, t; see Eq. 15. For this equality of momentum and impulse to be valid for any value of t′, it is required that

$$P_I(0,t')dt' = P_T(D,t'')dt''$$

or

$$P_T(D,t'') = P_I(0,t')/(dt''/dt'), \qquad (18)$$

where dt′′/dt′ is given by Eq. 16. It is noted that $P_T(D,t'')$ is assumed to vary smoothly from t''_{n+1} to t''_{n+2} *rather than with the short pulse* from t''_{n+1} to $t''_{n+1}+2(x_n-x_{n+1})/c$ that would occur if there were no high frequency damping due to viscosity; see Fig. 13 and, e.g., Landau and Lifshitz,[16] p. 300. For a given value of t′, the corresponding value of t′′ now can be calculated using Eq. 13 and the transmitted pressure at time t′′ then can be calculated using Eq. 18. Equation 18 shows that the pressure of the transmitted wave at time t′′ is reduced from that of the incident wave at the corresponding time t′ by

$$(dt''/dt')^{-1}.$$

For D = 0, there would be no reduction in the pressure of the incident wave because dt′′/dt = 1. However, for D > 0, there would be a reduction in the pressure of the incident wave because dt′′/dt′ > 1, as previously discussed. It is emphasized that there would be *no reduction* in the incident wave if the incident wave were *constant* in time because dt′′/dt′ = 1 in this case. This accentuates the fact that in this model all the reductions in the pressures of the incident shock wave are the result of it being a *decreasing* function of time.

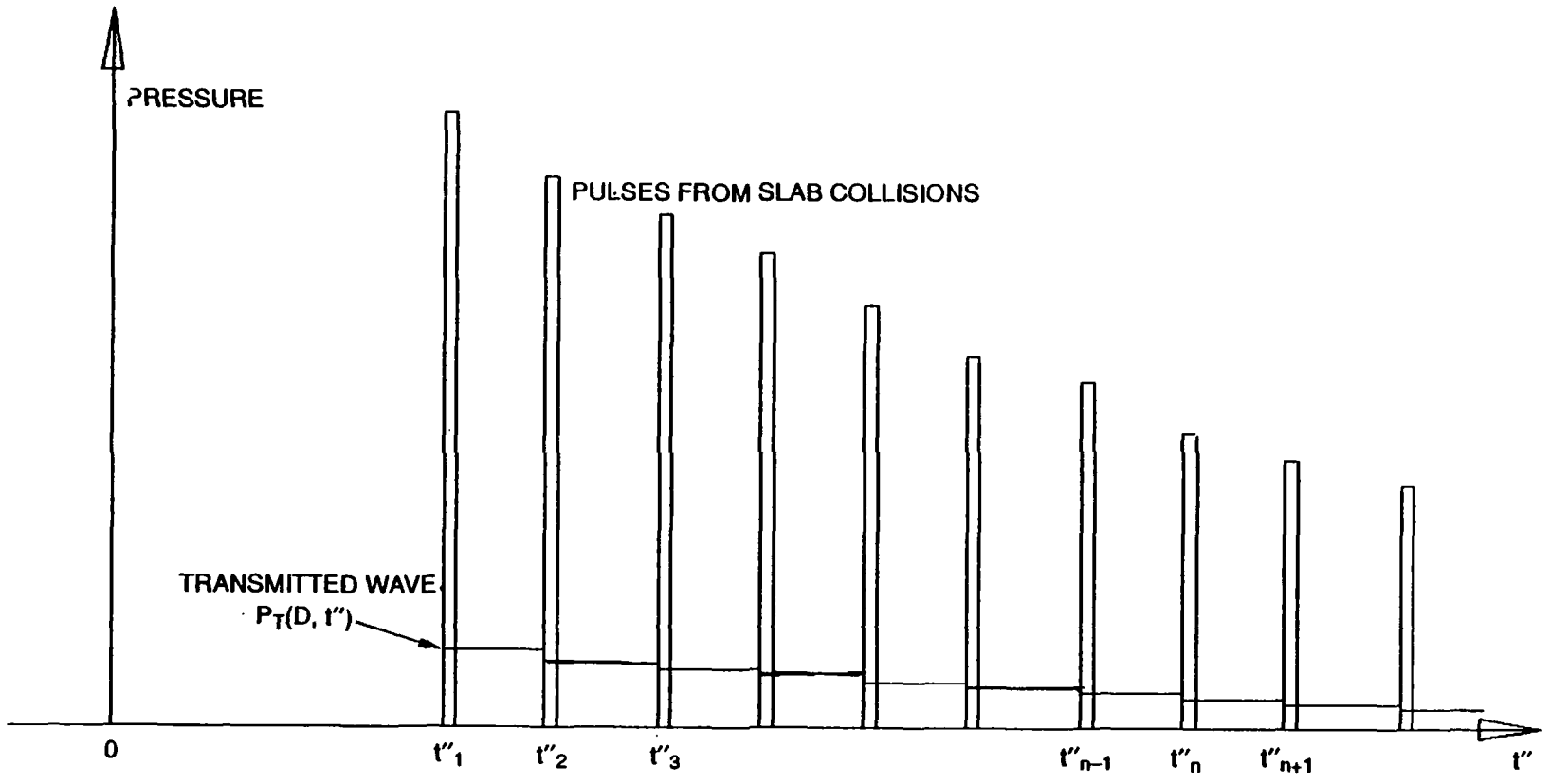

Fig. 13. Transmitted wave $P_T(D,t'')$ and pulses from slab collisions (schematic).

For a three-dimensional situation, the cavitated slabs are very unstable and would rapidly break up into droplets that would collide with the opposite side of the barrier. This would not result in much change in the velocities of the liquid in the slabs, but it would produce many more collisions and acoustic pulses that would be even more rapidly damped than in the one-dimensional case. This phenomenon would produce a smoother transmitted wave for a given slab thickness than that for the one-dimensional situation presented above.

ENERGY TRANSMISSION RATIO

The energy flux per unit area (i.e., the energy flux density) of the incident wave is determined using

$$E_I = (\rho c)^{-1}\int_0^{\infty}[P_I(0,t')]^2dt', \qquad (19)$$

see Cole,[15] p. 143. In like manner, the energy flux per unit area of the transmitted wave is determined using

$$E_T = (\rho c)^{-1}\int_0^{\infty}[P_T(D,t'')]^2dt''. \qquad (20)$$

Substituting Eq. 18 for P_T in Eq. 20, and using $dt'' = (dt''/dt')dt'$, gives

$$E_T = (\rho c)^{-1}\int_0^{\infty}[P_I(0,t')]^2(dt''/dt')^{-1}dt'. \qquad (21)$$

Equation 21 shows that the energy flux density of the transmitted

wave is *less* than that of the incident wave because $dt''/dt' > 1$; see the discussion of Eq. 16. The energy transmission ratio, E_T/E_I, now can be determined by using Eqs. 19 and 21. As explained above, the impulse of the transmitted wave is the same as that of the incident wave.

SPECIAL CASES

To demonstrate the use of this model, the special cases of the exponentially and hyperbolically decaying incident shock waves are now presented.

Case 1. Exponentially Decaying Incident Shock Wave

The pressure for the special case of an exponentially decaying incident shock wave is

$$P_I(0,t') = P_{I0}\exp(-t'/\theta), \tag{22}$$

where P_{I0} is the peak pressure (occurring at $t' = 0$) and θ is the exponential time decay constant. In this case, Eq. 16 becomes

$$\frac{dt''}{dt'} = 1 + \tfrac{1}{2}\rho cD \exp(t'/\theta)/(P_{I0}\theta)$$

$$= 1 + \tfrac{1}{2}D^*\exp(t'/\theta), \tag{23}$$

where

$$D^* = \rho cD/(P_{I0}\theta) \tag{24}$$

is the nondimensional barrier thickness. For a given value of t', the corresponding value of t'' now can be calculated using Eq. 13, and the transmitted pressure at time t'' then can be

calculated using Eqs. 18 and 23. For $t' = 0$

$$t'' = \tfrac{1}{2}\rho c D/P_{I0} = \tfrac{1}{2}D^*\theta \qquad (25)$$

and the initial (peak) pressure of the transmitted wave is

$$P_T(D,t'') = P_T(D,\tfrac{1}{2}D^*\theta) = P_{I0}/(1 + \tfrac{1}{2}D^*). \qquad (26)$$

Equation 26 shows that the peak pressure of the transmitted wave is *less* than that of the incident wave by a factor of $(1+\frac{1}{2}D^*)^{-1}$. For sufficiently large values of t', it can easily be seen from Eqs. 13 (for t''), 22 (for P_I), and 24 (for D^*) that

$$t'' \approx \tfrac{1}{2}D^*\theta \exp(t'/\theta) \qquad (27)$$

and, from Eqs. 18 and 23, that

$$P_T(D,t'') \approx 2P_{I0}D^{*-1} \exp(-2t'/\theta). \qquad (28)$$

For sufficiently large values of t'', Eqs. 27 and 28 imply that

$$P_T(D,t'') \approx \tfrac{1}{2}D^*(\theta/t'')^2 P_{I0}. \qquad (29)$$

Equation 29 shows that for large times the transmitted wave decays as the reciprocal of the square of the time. This is a much slower decay than that of the incident wave that decays exponentially with time.

From Eq. 19, the energy flux per unit area of the incident shock wave becomes

$$E_I = (\rho c)^{-1} P_{I0}^2\theta/2, \qquad (30)$$

and, from Eq. 21, the energy flux per unit area of the transmitted wave becomes

$$E_T = (\rho c)^{-1}\int_0^{\infty} P_{I0}^2 \exp(-2t'/\theta)[1+\tfrac{1}{2}D^* \exp(t'/\theta)]^{-1} dt', \quad (31)$$

by using Eq. 23. Substituting $t' = \theta \log_e u$ into Eq. 31 and dividing the result by Eq. 30, the energy transmission ratio for this case can be expressed as

$$E_T/E_I = \int_1^{\infty} 2(u^3 + \tfrac{1}{2}D^* u^4)^{-1} du. \quad (32)$$

From this equation, in the extreme situation where $D^* = 0$,

$$E_I/E_T = 1, \quad (33)$$

as expected. Also, in the extreme situation where D^* becomes arbitrarily large, it can be seen from Eq. 32 that

$$E_I/E_T = 4/(3D^*). \quad (34)$$

It can be easily verified for these two extreme situations (i.e., Eqs. 33 and 34) that the expression

$$(1 + 3D^*/4)^{-1}$$

has the same asymptotic behavior. Also, by numerically integrating Eq. 32, it can be shown that for $0 < D^*$

$$(1 + 3D^*/4)^{-1} - \delta < E_T/E_I < (1 + 3D^*/4)^{-1} ,$$

where* $\delta \approx 0.0261$. Thus, because of the correct asymptotic behavior and the small value of δ, it appears that for many purposes the approximation,

$$E_T/E_I \approx (1 + 3D^*/4)^{-1}, \qquad (35)$$

should be adequate for this case.

Thus, for the exponentially decaying incident shock wave, the peak pressure and energy flux density of the transmitted wave are reduced, but the transmitted wave does not decay as rapidly as does the incident wave. This is expected because the impulse of the transmitted wave is always equal to that of the incident wave for this model.

Case 2. Hyperbolically Decaying Incident Shock Wave

In the special case of a hyperbolically decaying incident shock wave,

$$P_I(0,t') = P_{I0}(1 + t'/\theta)^{-1}, \quad \text{for} \quad 0 \le t' < \tau \qquad (36)$$
$$= 0, \qquad \text{otherwise}$$

where, as in the previous special case, P_{I0} is the peak pressure (occurring at $t' = 0$), θ is the hyperbolic time decay constant (defined in analogous fashion to the previous special case) and τ is the cut-off time. In this case, Eq. 16 becomes

$$\frac{dt''}{dt'} = 1 + \tfrac{1}{2}D^*, \quad \text{for } 0 \le t' < \tau \qquad (37)$$

---

*Note that at $D^* = 0.48$, the numerical integration of Eq. 32 yields $E^T/E^I = 0.7092$. This is approximately equal to the lower bound (i.e., the left-hand side) of this inequality.

where D^* is defined to be the same as in Eq. 24. However, unlike the previous special case (Eq. 23), Eq. 37 is *constant* in time except for the discontinuity at $t' = \tau$. For this hyperbolically decaying shock wave, Eq. 13 becomes

$$\begin{aligned} t'' &= \tfrac{1}{2}D^*\theta + (1 + \tfrac{1}{2}D^*)t', \quad \text{for } 0 \le t' < \tau \\ &= \infty, \quad \text{for } t' \ge \tau \end{aligned} \tag{38}$$

and Eq. 18 becomes

$$\begin{aligned} P_T(D,t'') &= P_{I0}(1 + t'/\theta)^{-1}/(1 + \tfrac{1}{2}D^*), \quad \text{for } 0 \le t' < \tau \\ &= 0, \quad \text{otherwise.} \end{aligned} \tag{38a}$$

Solving for t' in Eq. 38 and substituting the resulting expression in Eq. 38a gives

$$\begin{aligned} P_T(D,t'') &= \frac{P_{I0}}{1 + \tfrac{1}{2}D^*}\left[\, 1 + \frac{t''-\tfrac{1}{2}D^*\theta}{\theta(1+\tfrac{1}{2}D^*)}\,\right]^{-1} \\ &= P_{I0}[1 + \tfrac{1}{2}D^* + (t'' - \tfrac{1}{2}D^*\theta)/\theta]^{-1} \\ &= P_{I0}(1 + t''/\theta)^{-1}, \quad \text{for } 0 \le t''-\tfrac{1}{2}D^*\theta < \tau(1+\tfrac{1}{2}D^*) \\ &= 0, \quad \text{otherwise.} \end{aligned} \tag{39}$$

For this case Eq. 39 shows that when $0 \le t''-\tfrac{1}{2}D^*\theta < \tau(1+\tfrac{1}{2}D^*)$, *the transmitted wave has the same form as the incident wave*; see Eq. 36. However, because the pressure of the transmitted wave is zero for $t'' < \tfrac{1}{2}D^*\theta$, *the peak pressure of the transmitted wave is decreased. Also, the duration in increased.* The transmitted wave is attenuated in this fashion.

For the hyperbolically decreasing shock wave, Eq. 19 becomes

$$E_I = (\rho c)^{-1} P_{I0}^2 \theta [1 - (1 + \tau/\theta)^{-1}], \qquad (40)$$

Eq. 21 becomes

$$E_T = (\rho c)^{-1} P_{I0}^2 \theta [1 - (1 + \tau/\theta)^{-1}]/(1 + \tfrac{1}{2}D^*), \qquad (41)$$

and the energy transmission ratio becomes

$$E_T/E_I = (1 + \tfrac{1}{2}D^*)^{-1}. \qquad (42)$$

Note that this ratio is independent of τ. Comparing Eq. 42 with Eq. 35 shows that the energy transmission ratio for the hyperbolically decreasing shock wave is greater than that of the exponentially decreasing shock wave.

LOWER PRESSURE INCIDENT SHOCK WAVES

The theoretical development that was presented above can be easily extended to the problem of incident shock waves with lower pressures and barriers with *finite* pressures. This can be accomplished with simple modifications of Eqs. 1-8 to treat cavitated slabs with *finite* thicknesses, assuming that the liquid cavitates at a definite pressure. However, the situation could be much more complicated because one must explicitly consider the dynamics of the growth of the cavitation bubbles and the effect of impurities (and their statistical distributions) and other phenomena; see, e.g., Prosperetti.[17] Also, the treatment of the transmitted pulse can be easily modified in a similar fashion. Of course, for sufficiently low pressure shock waves that are

incident on a barrier that contains material, the usual acoustic treatment of sound wave reflection and transmission can be applied; see, e.g., Landau and Lifshitz,[16] p. 253. However, these modifications require more input parameters and might not be of much practical use because protection is most important for incident shock waves with very high pressures. Although this phenomenon should scale for sufficiently high pressures, it might not scale for low pressures. This is because the effect of surface tension and viscosity might be very important during cavitation and collision for sufficiently low pressures.

EXTENSION OF MODEL TO THREE DIMENSIONS

Perhaps the most elementary three-dimensional extension of the evacuated-barrier cavitation model is a model of an incident shock wave emanating from an explosion that can be considered as a point source. It is noted that this situation might only be two-dimensional because of possible axial symmetry about the line from the point source to the nearest point on the barrier. For this situation, a simple model can be applied for the initial velocity distribution after the cavitation (as shown in Fig. 9) for the interaction of an incident shock wave with an *arbitrary angle of incidence;* see, e.g., Waldo[14] and cf. Eq. 7.

Using this velocity distribution, the pressure history on the opposite side of the barrier can be determined by employing the same concepts that were developed previously for the one-dimensional situation in the evacuated-barrier cavitation model. The calculation of the pressure history for any distance *beyond* the opposite side of the barrier would require a solution of the

acoustic wave equation. The boundary condition for this solution is the pressure history at each location on the opposite side of the barrier (as calculated using the model for arbitrary angles of incidence that was described previously). However, even without explicitly solving this problem, it appears to be reasonable that the pressures on the opposite side of the barrier would rapidly decrease for locations with increasing angle of incidence. This would mean that the pressures of the transmitted wave would rapidly decrease with increasing distances beyond the opposite side of the barrier (even along the line of normal incidence of the shock wave, i.e., the axis of symmetry). Thus, it can be speculated that there would be a decrease in the impulse of the transmitted shock wave at a given location from what it would have been at that location if there were no barrier. However, a full treatment of the problem would be necessary to justify this speculation.

For explosions that are not close to the barrier, the bubble that is produced by the explosion will have most of its expansion take place considerably after the shock wave interaction. Cole,[15] p. 312, has shown that a bubble will be repelled by a free surface such as that at the evacuated barrier and will be attracted by an rigid surface. Thus, it is plausible that the bubble repulsion by the evacuated barrier will reduce the effect of the shock wave that emanates from the collapse of the bubble simply because the collapse occurs further away than if the evacuated barrier were not present. Also the pressure of the transmitted shock wave produced by the collapse of the bubble is

reduced by the same effect as was modeled in the development previously, see Eqs. 13, 16 and 18. Unfortunately, a circumstance might occur in which the explosion is too close to the barrier, the barrier is not sufficiently thick, and the object to be protected by the barrier is too close to the opposite side of the barrier. In this circumstance, the bubble expansion might be sufficiently large to penetrate the barrier and to interact with the object. If the object is solid and cannot have much movement, the bubble could be attracted to the barrier and collapse on the object. This collapse could cause unacceptable damage to the object. However, even in this circumstance the damage could be substantially reduced by the presence of the barrier.

EXTENSION OF MODEL TO BARRIERS CONTAINING MATERIAL

Consider a barrier containing a material of very low density and very low crushing-resistance pressure. It is plausible that the reductions in the pressures of the transmitted shock waves caused by this barrier could be about the same as those for an evacuated barrier. However, the thickness of this evacuated barrier would be *less* than the actual thickness of the barrier containing the material. This "effective thickness" might be equal to that of the vacant space remaining in the barrier if the material were compressed so that it would have a mass density that is equal to that of the liquid. Such materials might include gasses (e.g., air, carbon dioxide, water vapor or steam, etc.), foams (see, e.g., Kudinov et al.[9,10] and Lyakhov,[11]), bubble screens, styrofoam, solid foams made of elaborate composite materials, some complicated combination of materials, or

layers of materials. However, it would not be surprising if the reductions of pressures in the transmitted shock waves were greater than those predicted by an evacuated barrier with an effective thickness obtained in this manner. The greater reductions might occur because of the (possible) absorption of the incident shock wave energy by the material in the barrier. Also it is possible that the barrier could be behaving as if it were evacuated throughout its full unadjusted thickness, without the adjustment of the thickness as described. Of course, it is possible that a barrier could allow more energy transmission than that of the evacuated-barrier cavitation model. More energy transmission would occur in the trivial case where the barrier is filled with the same liquid as that outside the barrier. In this case there would be no change in the transmitted shock wave from that of the incident shock wave.

More dense materials (e.g., steel, concrete, sand, etc.) might reflect a substantial amount of the energy of the incident shock wave and reduce the pressures of the transmitted shock wave. But barriers composed of such dense materials are frequently impractical. Of course, more elaborate mathematical models of the interaction of shock waves with barriers composed of various materials can be formulated using the concepts considered in the evacuated-barrier cavitation model. Also, further considerations such as the drag forces on the liquid droplets as they move across the barrier might be included. A simple barrier with negligible mass density that uniformly crushes with a constant pressure can be easily treated using the concepts in Ref.14.

EXPERIMENTS TO TEST THE THEORY

To test this theory, see Eqs. 13, 16, and 18, experiments could be performed for a one-dimensional evacuated barrier by using an underwater shock tube. Also, calculations using the theory could be compared with existing data for bubble screens and low-density foams. It would not be expected that these calculations would agree precisely with the data. But it is plausible that the evacuated-barrier model, with an effective thickness (as previously discussed), might provide a good first approximation.

POSSIBLE APPLICATIONS

Because almost all damaging shock waves decay with time (Cole,[15] p. 110), the evacuated-barrier concept could be used to protect surface ships and submarines by encasing the hull with a very low density solid foam (as previously discussed). However, this foam would have to be strong enough to withstand conditions at sea. In addition, for submarines the foam would have to resist the pressures at the collapse depth of their pressure hulls. Such foams might add too much to the size and weight of the vessel to be practical.

It is conceivable that a bubble screen could be employed for naval ships and submarines during an attack. However, the problems of additional piping and supply of the gas for the bubbles would have to be surmounted. Steam from the boilers could be

used if enough could be generated without severely hindering the mobility of the craft. Also, a chemical could be released by the craft that would react with the water and form bubbles that could provide an effective screen. This chemical could be injected into the water as coated pellets at the bow of the craft when under attack. The coatings would dissolve at different times and thus the chemical would react at different times. This would provide a bubble screen for the full length of the hull.

There are many other schemes that could be investigated, and numerous industrial applications of bubble screens such as the protection of underwater structures from explosions during construction and demolition.

Note that because the impulse is not reduced by the barrier (see the discussion preceding Eq. 18), there might not be much reduction in damage imparted to equipment that responds mainly to impulse rather than peak pressure or energy flux density. As previously discussed, the bubble produced by the explosion might collapse on the barrier, penetrate it, and cause additional damage. However, because of the low density of the barrier, the bubble might be repelled by it and not penetrate the barrier; see, e.g., Cole,[15] pp. 312-352.

SUMMARY

The evacuated-barrier cavitation model was developed. In this model a one-dimensional shock wave in a liquid is incident on the surface of an evacuated barrier. Because of this interaction, the liquid cavitates. The slabs of cavitated liquid subsequently move across the barrier and collide with the liquid

surface on the opposite side of the barrier. These collisions produce a high frequency of pulses in the liquid on the opposite side of the barrier that are rapidly damped out. The pressures and energy flux density of the resulting wave that is transmitted into the liquid on the opposite side of the barrier can be considerably reduced. These reductions are the result of the fact that the decay in the pressure of the incident shock wave causes the distances between the cavitated slabs to spread as they move across the barrier. Spreading causes the transmitted wave to have lower pressures and longer duration than the incident shock wave. The impulse of the transmitted wave is the same as that of the incident wave. The pressure history of the transmitted wave can be determined for a decreasing incident wave using Eqs. 13, 16, and 18. For the important case of an exponentially decaying shock wave, the peak pressure of the transmitted wave is given by Eq. 26 and the energy flux density of the transmitted wave can be determined using Eq. 32 or its approximate form, Eq. 35. For a hyperbolically decaying incident shock wave it was shown (Eq. 39) that the transmitted wave function has the *same form* as that of the incident wave but is attenuated. Extensions of the evacuated-barrier cavitation model to treat three-dimensional situations and to include various materials within the barrier were discussed. Applications of the model for the shock protection of surface ships and submarines as well as industrial applications were considered.

THIS PAGE INTENTIONALLY LEFT BLANK

REFERENCES

1. van Wijngaarden, L., "On the Structure of Shock Waves in Liquid-Bubble Mixtures," Appl. Sci. Res., Vol. 22, pp. 366-381 (Jul 1970).

2. van Wijngaarden, L., "One-Dimensional Flow of Liquids Containing Small Gas Bubbles," Annual Reviews of Fluid Mechanics, Vol. 4, pp. 369-396 (1972).

3. Ng, K.C., and L. Ting, "Wave Propagation Through a Thin Bubbly Layer," J. Acoust. Soc. Am., Vol. 79, pp. 924-926 (Apr 1986).

4. Crespo, A., "Sound and Shock Waves in Liquids Containing Bubbles," The Physics of Fluids, Vol. 12, pp. 2274-2282 (1969).

5. Campbell, I.J., and A.S. Pitcher, "Shock Waves in a Liquid Containing Gas Bubbles," Proc. Royal Soc., Part A, Vol. 243, pp. 534-545 (1958).

6. Batchelor, G.K., "Compression Waves in a Suspension of Gas Bubbles in Liquid," Fluid Dynamics Transactions, Vol. 4, pp. 425-445 (1969).

7. Kuznetsov, V.V., V.E. Nakoryakov, B.G., Pokusaev and I.R. Shreiber, "Propagation of Perturbations in a Gas-Liquid Mixture," J. Fluid Mech., Vol. 85, part 1, pp. 85-96 (1978).

8. Sheynina, S.I., "Effectiveness of the Response of an Air Fence to Application of a Time-Varying Pressure to the Surface of a Body of Water," Fluid Mechanics-Soviet Research, Vol. 15, pp. 115-125 (Sep-Oct 1986).

9. Kudinov, V.M., B.I. Palamarchuk, B.E. Gel'fand, and S.A. Gubin, "Parameters of Shock Waves in the Detonation of Explosive Charges in Foam," Soviet Physics Doklady, Vol., 21, pp. 256-258 (May 1976).

10. Kudinov, V.M., B.I. Palamarchuk, S.G. Lebed', A.A. Borisov, and B.E. Gel'fand, "Propagation Characteristics of Detonation Waves in Aquamechanical Foam Formed by a Combustible Gas Mixture," Soviet Physics Doklady, Vol. 22, pp. 247-248 (May 1977).

11. Lyakhov, A.G., "The Effect of Separation due to Cavitation on the Extinction of Waves in a Liquid with Porous Interlayers," Zhurnal Prikladnoi Mekhaniki i Tekhnicheskoi Fiziki, Vol. 30, pp. 134-139 (Nov-Dec 1989).

12. Kennard, E.H., "Explosive Load on Underwater Structures as Modified by Bulk Cavitation," David Taylor Model Basin Report 511 (1943).

13. Cushing, V., "Study of Bulk Cavitation and Consequent Water Hammer," Engineering-Physics Company Final Report on Contract NONR-3389(00) EPCO Project 106 (Oct 1961).

14. Waldo, Jr., G.V., "A Bulk Cavitation Theory with a Simple Exact Solution," Naval Ship Research and Development Center Report 3010 (Apr 1969).

15. Cole, R.H., "Underwater Explosions," Dover Publications, Inc., New York (1948).

16. Landau, L.D., and E.M. Lifshitz, "Fluid Mechanics," Addison-Wesley Publishing Company, Inc., Reading, Mass. (1959).

17. Prosperetti, A., "Physics of Acoustic Cavitation," Frontiers in Physical Acoustics, Soc. Italiana di Fisica, Bologna, Italy (1986).

THIS PAGE INTENTIONALLY LEFT BLANK

INITIAL DISTRIBUTION

Copies		
1	ONR	
	10P6	W. Lukens
1	ONT	
	20T	P. Quinn
2	NAVSEA	
	1	Library
	1	55X11 R. McCarthy
1	DNA	
	SPSD	C. Nofziger
1	NAVPGSCOL	
	Library	
1	NUSC	
	Technical Library	
1	NAVWARCOL	
1	NAVSHIPYD BREM	
	Library	
1	Library of Congress	
	Science and Tech Div	
2	Maritime Administration	
	1	Office of Maritime Tech
	1	Div of Naval Arch
1	USNA	
	Technical Library	
12	DTIC	
1	NASA	
	Scientific and Tech Information Facility	

CENTER DISTRIBUTION

Copies	Code	Name
1	01	R.E. Metrey
1	01ATD	D. Sheridan
1	0111	D.J. Clark
3	0112	B. Douglas
1	12	G.D. Kerr
1	15	W.B. Morgan
1	154	J.H. McCarthy
1	1542	T. Huang
1	17	M.A. Krenzke
1	172R	
1	1702	J. Corrado
1	172	R. Rockwell
2	172.4	A. Wiggs N. Gifford
1	174	I.S. Hansen
2	174.4	S.L. Wang H.P. Gray
1	175	J.W. Sykes
14	175.1	B. Whang C.D. Bond W.E. Gilbert W.D. Gottwald C.D. Milligan C.Q. Nguyen F. Rasmussen J.M. Ready B.S. Rose P.N. Roth Y.G. Sohn C.W. Tinker T.G. Toridis S. Zilliacus

INITIAL DISTRIBUTION (Continued)

CENTER DISTRIBUTION (Continued)

Copies	Code	Name
1	175.2	W.R. Conley
1		R.E. Baker
1		L. Chrysostom
1		K.A. Dodd
1		P.J. Dudt
1		D.P. Hagar
1		H.P. Hashmall
1		L.R. Hill
1		M.W. Hoffman
1		P.A. Manny
1		M.A. Neff
1		C.S. Stuber
20		G. Waldo, Jr.
1		S.C. Walter
1	177	R. Fuss
3	177.1	M. Riley F. Costanzo J. Gordon
1	177.2	J. Krezel
1	19	M. Sevik
1	191	C.P. Henson
1	1912	R.J. Rahman
1	195	J.R. Spina
1	196	D. Vendittis
1	1962	A. Kilcullen
1	1965	J.M. Niemiec
1	28	G.A. Wacker
1	284	E.C. Fischer
1	2844	V. Castelli

CENTER DISTRIBUTION (Continued)

Copies	Code	Name
1	3421	TIC(C)
1	3422	TIC(A)
1	3431	Office Services
10	3432	Reports Control